Effects of dispersion forces on the structure and thermodynamics of fluid krypton

N. Jakse,[1] J. M. Bomont,[1] I. Charpentier,[2] and J. L. Bretonnet[1]
[1]*Laboratoire de Théorie de la Matière Condensée, Université de Metz, 1, boulevard F. D. Arago, CP 87811, 57078 Metz Cedex 3, France*
[2]*Laboratoire de Modélisation et de Calcul, Institut de Mathémathiques Appliquées de Grenoble, CNRS, BP 53, 38041 Grenoble Cedex, France*
(Received 1 December 1999)

Semianalytical and numerical calculations are performed to predict the structural and thermodynamic properties of low-density Kr fluid. Assuming that the interatomic forces can be modelled by a pairwise potential plus the three-body Axilrod-Teller potential, two different routes are explored. The first one is based on the hybridized mean spherical approximation integral equation of the theory of liquids and the second one uses large-scale molecular dynamics (MD). Algorithms for MD simulation are constructed on parallel machines to reduce the amount of computer time induced by the calculations of the three-body forces and the pair-correlation function. Our results obtained with the two methods mentioned above are in quite good agreement with the recent small-angle neutron-scattering experiments [Formisano *et al.*, Phys. Rev. Lett. **79**, 221 (1997); Benmore *et al.*, J. Phys.: Condens. Matter **11**, 3091 (1999)]. Moreover, the reliability of the asymptotic form of the integral equation is assessed for the specific case of dispersion forces including the three-body contributions, by an analysis at low wave vector and low density. It is seen that the effects of the Axilrod-Teller triple-dipole potential cannot be ignored to describe the structure and the thermodynamic properties of fluid krypton even at low density.

PACS number(s): 61.20.−p, 51.30.+i

I. INTRODUCTION

One of the fundamental tasks of liquid theory is to elucidate the basic interactions to be used as a starting point for development of statistical-mechanical models. For simple fluids, extensive studies have shown that the Lennard-Jones 12-6 potential (LJ) is a satisfactory effective pair potential though the true one is certainly not of the 12-6 form. So, using all available sources of information from experimental observations for noble gases, Aziz and Slaman [1] have derived an empirical pair potential, which includes only two-body corrections to the London dispersion energy arising from the multipole expansion. Such a description is not strictly valid because the interaction between two particles depends on the presence of a close third one, and at least three-body interactions coming from the third-order perturbation have to be taken into account. Different ways of handling such three-body contributions have been explored for many years [2]. For instance, Barker, Fisher, and Watts [3] have proposed a pair potential suitable for the physical properties of liquid argon, in which three-body and quantum corrections have been included, and more recently, Barker [4] has built a pair potential with many-body effects that is devoted to liquid krypton and xenon. Besides, following the idea of Casanova *et al.* [5], Reatto and Tau [6] proposed to complete the two-body interactions in noble gases by adding the three-body contribution of Axilrod-Teller [7] through a state-dependent effective pair potential.

A direct probe of the interaction potential is possible through the use of the density fluctuations, which is obtained from the static structure factor $S(q)$ or equivalently from the pair-correlation function $g(r)$ [8]. Besides, it has been demonstrated that the small-q behavior of $S(q)$, between 0.5 and 5 nm^{-1}, can yield the reliability of the long-range interactions. Those last four years, precise measurements of $S(q)$ at small scattering angles have been performed on fluid Ar and Kr, which allowed the extraction of not only the C_6 coefficient of the London dispersion potential [9,10], but also the strength of the three-body potential for Kr, assumed to be of the Axilrod-Teller form [11,12]. This detection represents certainly the most unequivocal evidence of the presence of three-body forces in condensed matter (at least in their long-range part) and supports the fact that these cannot be ignored. Therefore, the experimental structure of Kr at small scattering angle provides a stringent test for theoretical calculations dealing with three-body forces.

The purpose of this paper is to extend the previous theoretical work [13] on the structure of fluid Kr at low q to the thermodynamic properties at several temperatures. This is performed by using two different methods. On one hand, we have used a thermodynamically consistent integral equation, called hybridized mean spherical approximation (HMSA) [14,15], extended to include the three-body interactions [13]. On the other hand, we have carried out molecular-dynamics (MD) simulations involving 6912 and 16384 particles, thanks to an efficient algorithm for parallel computers [16] in order to calculate accurate structure factor at small scattering angles. To describe the interactions between Kr atoms in the present paper, we combine the true pair potential of Aziz-Slaman [1] with the Axilrod-Teller triple-dipole one [7], by means of a state-dependent effective pair potential. A comparison with the experimental data of structure and thermodynamics allows us to test either the models of interaction or the HMSA.

II. MODELS AND SIMULATION

A. Effective interatomic potential

We assume that the interatomic interaction in Kr consists of a N-body potential-energy function, constructed via a true pair potential u_2 plus a three-body potential u_3

$$U_N(\mathbf{r}_1,\ldots,\mathbf{r}_N)=\sum_{i<j}^{N} u_2(\mathbf{r}_i,\mathbf{r}_j)+\sum_{i<j<k}^{N} u_3(\mathbf{r}_i,\mathbf{r}_j,\mathbf{r}_k). \quad (1)$$

Neglecting terms after the third-order one appears to be a reasonable approximation [2] for the physical properties under study. As u_2, we select Aziz and Slaman's (AS) [1] pair potential that reads

$$u_2(x_{ij})=A\exp(-\alpha x_{ij}+\beta x_{ij}^2)-F(x_{ij})\sum_{j=0}^{2}\frac{C_{2j+6}}{2j+6}, \quad (2)$$

where $x_{ij}=r_{ij}/\sigma$ is the reduced distance and σ the position of the node of the potential. According to the authors, the repulsive and attractive parts have to be matched with the switching function

$$F(x_{ij})=\begin{cases}\exp\left[-\left(\dfrac{D}{x_{ij}}-1\right)^2\right] & \text{if} \quad x_{ij}<D,\\ 1 & \text{if} \quad x_{ij}\geqslant D.\end{cases} \quad (3)$$

The relevant parameters in Eqs. (2) and (3) are listed in the paper of Aziz and Slaman [1]. As u_3, we use the usual expression derived by Axilrod-Teller (AT) [7]

$$u_3(\mathbf{r}_i,\mathbf{r}_j,\mathbf{r}_k)=\nu\frac{1+3\cos\theta_i\cos\theta_j\cos\theta_k}{r_{ij}^3r_{ik}^3r_{jk}^3}, \quad (4)$$

which corresponds to an irreducible triple-dipole potential between closed-shell atoms. The value of the strength ν is 2.204×10^{-26} J nm^9 for Kr, and θ_i, θ_j, and θ_k denote, respectively, the angles at vertex i, j, and k of the triangle (i, j, k) with sides $r_{ij}=|\mathbf{r}_j-\mathbf{r}_i|$, $r_{ik}=|\mathbf{r}_k-\mathbf{r}_i|$, and $r_{jk}=|\mathbf{r}_k-\mathbf{r}_j|$.

In performing the molecular-dynamics calculations, it is also necessary to consider the force acting on a particle i from a particle j, which is derived from the AS potential under the form

$$\mathbf{F}_{ij}(x_{ij})=\Bigg\{A\exp(-\alpha x_{ij}+\beta x_{ij}^2)(-\alpha+2\beta x_{ij})-F(x_{ij})\times\Bigg[\sum_{j=0}^{2}\frac{(2j+6)C_{2j+6}}{x_{ij}^{2j+7}}-\frac{2D(D-x_{ij})}{x_{ij}^3}\sum_{j=0}^{2}\frac{C_{2j+6}}{x_{ij}^{2j+6}}\Bigg]\Bigg\}\mathbf{e}_{ij}, \quad (5)$$

where $\mathbf{e}_{ij}$ is a unit vector in the $\mathbf{r}_{ij}$ direction. For the AT potential, the force acting on the particle i from the particles j and k is given by

$$\mathbf{F}_{i,jk}(r_{ij},r_{jk},r_{ik})=\frac{\partial u_3}{\partial r_{ij}}\mathbf{e}_{ij}+\frac{\partial u_3}{\partial r_{ik}}\mathbf{e}_{ik}, \quad (6)$$

while the forces acting on j and k are, respectively,

$$\begin{cases}\mathbf{F}_{j,ik}(r_{ij},r_{jk},r_{ik})=-\dfrac{\partial u_3}{\partial r_{ij}}\mathbf{e}_{ij}+\dfrac{\partial u_3}{\partial r_{jk}}\mathbf{e}_{jk},\\ \mathbf{F}_{k,ij}(r_{ij},r_{jk},r_{ik})=-\dfrac{\partial u_3}{\partial r_{ik}}\mathbf{e}_{ik}-\dfrac{\partial u_3}{\partial r_{jk}}\mathbf{e}_{jk}.\end{cases} \quad (7)$$

The standard expressions of the three partial derivatives of u_3 can be found in the paper of Hoheisel [17].

B. Hybridized mean spherical approximation

The calculations of the structural and thermodynamic properties are performed by using the HMSA that is briefly described below. As attested in the literature [5,6,18,19,20], the basic assumption in this approach is that the three-body potential reduces to a state-dependent effective pair potential written as

$$u(r_{ij})=u_2(r_{ij})+\langle u_3(r_{ij})\rangle, \quad (8)$$

with

$$\langle u_3(r_{ij})\rangle=-\frac{\rho}{\beta}\int g(r_{ik})g(r_{jk})\times[\exp\{-\beta u_3(\mathbf{r}_i,\mathbf{r}_j,\mathbf{r}_k)\}-1]d\mathbf{r}_k. \quad (9)$$

ρ is the number density, $\beta(=1/k_BT)$ the inverse temperature, and k_B is Boltzmann's constant.

If the interactions are given in terms of the effective pair potential $u(r_{ij})$, the integral equation theory provides a scheme to yield $g(r_{ij})$, which has reached nowadays a high degree of accuracy with the HMSA integral equation [14]. The latter combines the Ornstein-Zernike (OZ) equation

$$g(r_{ij})-1=c(r_{ij})+\rho\int[g(r_{ik})-1]c(r_{jk})d\mathbf{r}_k, \quad (10)$$

where $c(r_{ij})$ is the direct correlation function, with an approximate closure that reads

$$g(r_{ij})=\exp[-\beta u^R(r_{ij})]\left\{1+\frac{\exp[f(r_{ij})\{g(r_{ij})-1-c(r_{ij})-\beta u^A(r_{ij})\}]-1}{f(r_{ij})}\right\}. \quad (11)$$

Here, the assumption is made that the effective pair potential [Eq. (8)] may be split into a repulsive short-range part $u^R(r_{ij})$, and a weak attractive long-range part $u^A(r_{ij})$, according to the prescription of Weeks, Chandler, and Andersen [21]

$$u^R(r_{12})=\begin{cases}u(r_{12})-u(r_m) & \text{if} \quad r_{12}<r_m,\\ 0 & \text{if} \quad r_{12}>r_m,\end{cases} \quad (12)$$

$$u^A(r_{12})=\begin{cases}u(r_m) & \text{if} \quad r_{12}<r_m,\\ u(r_{12}) & \text{if} \quad r_{12}>r_m,\end{cases} \quad (13)$$

where r_m is the location of the minimum of the potential well. The term $f(r_{ij})$ is a mixing function whose expression is that of Bretonnet and Jakse [15], and which ensures the thermodynamic self-consistency in requiring the equality between the compressibilities coming from the viral equation of state and grand-canonical ensemble, namely,

$$\rho k_B T \chi_T = S(0), \tag{14}$$

where $S(0)$ stands for the long-wavelength limit of the structure factor. Therefore, Eqs. (8) to (14) are solved in a thermodynamically self-consistent manner. The solution of the HMSA integral equation is obtained by the classical algorithm proposed by Labik, Malijevski, and Vonka [22], which consists in solving the nonlinear set of equations with the traditional iterative technique [23]. A good accuracy of $S(q)$, especially at small q, is achieved when the functions are represented by a grid size of 1024 with a mesh of 0.02.

The HMSA discussed above includes automatically the calculation of the following thermodynamic properties due to the self-consistent condition (14). When three-body forces are assumed, the excess internal energy, the equation of state, and the isothermal compressibility are given, respectively, by [20]

$$\frac{U^{ex}}{\langle N \rangle} = \frac{\rho}{2!} \int u_2(r_{ij}) g(r_{ij}) d\mathbf{r}_{ij} + \frac{\rho^2}{3!} \int d\mathbf{r}_{ij} d\mathbf{r}_{ik} g^{(3)} \times (\mathbf{r}_{ij}, \mathbf{r}_{ik}) u_3(\mathbf{r}_{ij}, \mathbf{r}_{ik}), \tag{15}$$

$$p = \rho k_B T - \frac{\rho^2}{2!3} \int g(r_{ij}) \mathbf{r}_{ij} \cdot \nabla_{\mathbf{r}_{ij}} u_2(r_{ij}) d\mathbf{r}_{ij} - \frac{\rho^3}{3!3} \int d\mathbf{r}_{ij} d\mathbf{r}_{ik} g^{(3)}(\mathbf{r}_{ij}, \mathbf{r}_{ik}) \nabla_{\mathbf{r}_{ij}} u_3(\mathbf{r}_{ij}, \mathbf{r}_{ik}), \tag{16}$$

$$\chi_T = \frac{1}{\rho} \left(\frac{\partial \rho}{\partial p} \right)_T. \tag{17}$$

These expressions are formally exact and each of them contains explicitly the two- and three body terms, which depend on the pair and triplet distribution functions $g(r_{ij})$ and $g^{(3)}(\mathbf{r}_{ij}, \mathbf{r}_{ik})$. In practice, the three-particle distribution function is unknown and has to be approximated. In this work, the Kirkwood superposition approximation [24] is used

$$g^{(3)}(\mathbf{r}_{ij}, \mathbf{r}_{ik}) = g(r_{ij}) g(r_{ik}) g(r_{jk}) \exp[-\beta u_3(\mathbf{r}_{ij}, \mathbf{r}_{ik})]. \tag{18}$$

It is noticeable that the viral pressure remains exact to third order in density when this approximation is set.

C. Molecular dynamics

In order to reach the small-q range of $S(q)$, we are compelled to carry out large-scale molecular-dynamics simulations in the microcanonical ensemble (*NVE*). We deal with the individual motion of $N=6912$ pointlike particles situated in a cubic box. The latter is subject to the usual periodic boundary conditions, whose volume V is fixed to get the desired number density ρ. The equations of motion are integrated in a discrete form by means of a finite difference method [25], using the convenient Verlet's algorithm in the velocity form. The time step is $\Delta t = 10^{-15}$ s, and $g(r)$ is extracted over a sample of 8000 time-independent configurations every $10\Delta t$.

The calculation of the forces at each time step is one of the most demanding tasks. Since $\mathbf{F}_{ij} = -\mathbf{F}_{ji}$, for the two-body forces, and $\mathbf{F}_{i,jk} = -\mathbf{F}_{j,ik} - \mathbf{F}_{k,ij}$, for the three-body forces, the forces can be calculated once only leading to a computation time reduced roughly by a factor of 2. In addition, taking advantage of the short-ranged potentials that allow the use of cutoff radii, we use the linked-cell lists [26] in order to reduce the complexity of computations to $O(N)$, because only pairs and triplets of particles within the cutoff radius r_c are taken into account [27]. In our case, r_c equals 2.5σ for two- and three-body forces.

Nevertheless, for large-scale simulations, involving typically $N > 10^3$ particles, the execution time is still large. Thus, algorithms suitable for parallel computers are nowadays commonly used [28], and applied to liquid state studies [29]. Recently, we have built an algorithm based on a spatial decomposition (SD) method [30] that equally distributes the computation among the processors of the parallel machine. The SD method consists in dividing the simulation box into P regions. Each of them is assigned to a processor that performs the calculations for the particles situated in it and communicates the data to the other processors. Our program, in which the calculations of the forces and the pair-correlation function are parallelized, reduces the execution time by a factor RP where $R = t_1/(Pt_P)$ is the speedup, t_1 and t_P being, respectively, the execution time with 1 and P processors. For this purpose, the plate decomposition associated with a torus communication scheme has been used [16,30] with $N = 6912$ particles and $P = 6$ processors. We also used $N = 16384$ with $P = 8$ processors to show that our results become insensible for system sizes beyond $N = 6912$. In both cases, R takes values around 0.95.

III. RESULTS AND DISCUSSION

The HMSA and molecular dynamics have been used to study the physical properties of fluid Kr at temperatures and densities for which experimental results are available. In the first paragraph, the reliability of the interaction scheme is assessed by comparing the structure factor obtained by both theoretical routes to the measurements of Formisano *et al.* [10]. Then, in the two subsequent paragraphs, we study the structural behavior at low q and low density in order to deduce reliable information on the two- and three-body interactions from the structure. The objective is to access to a direct comparison with the experiment at the three-body level as suggested by Benmore *et al.* [11] and Guarini *et al.* [12].

A. Structural properties

The first step of our paper concerns the calculation of the structure of fluid Kr for $T = 297$ K and four different densities in the range between 1.52 and 4.277 nm^{-3}, corresponding to the thermodynamic states studied by Formisano *et al.* [10] and Guarini *et al.* [12]. Since these authors have performed their experiments only at small neutron-scattering angle, for the sake of expediency we present the results of

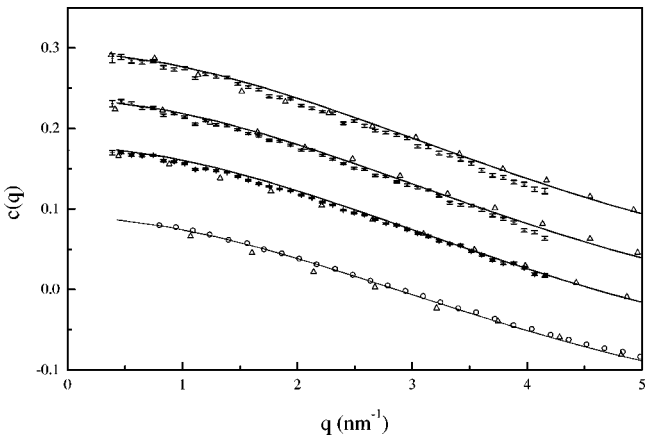

FIG. 1. Direct correlation function $c(q)$ for $T=297\,\mathrm{K}$, at $\rho=1.52$, 1.97, 2.42, and 4.277 nm^{-3} from the top to the bottom (the curves for $\rho=1.52$, 1.97, and 2.42 nm^{-3} are shifted upwards by an amount of 0.05, 0.1, and 0.15, respectively), calculated with the HMSA integral equation (solid line) and molecular dynamics (up triangles) by using Aziz and Slaman's pair potential plus the Axilrod-Teller three-body contribution. Crosses with error bars correspond to the experimental data of Formisano *et al.* [10], while open circles stand for those of Guarini *et al.* [12].

the Fourier transform of the direct correlation function $c(q)=[S(q)-1]/\rho S(q)$ at low q, rather than those of the structure factor $S(q)$.

Figure 1 displays the curves of $c(q)$. It is seen that the theoretical results, obtained by MD and HMSA with the AS plus AT potentials, are in excellent agreement with the experimental data. For the sake of clearness, the curves calculated with the two-body potential alone are not shown, nevertheless the MD and the HMSA curves compare also quite well together. While the AT contribution is included by means of an effective pair potential given by Eq. (8) in the HMSA, it is used under its original form owing to Eqs. (6) and (7) in MD. This demonstrates that the treatment of the three-body potential in the integral equation is valid in this range of densities. In our previous paper [13], we showed the relative role of the three-body contribution using the HMSA, by comparing the results obtained with the AS potential alone to those obtained with the combination of AS and AT potentials. The effect of the three-body contribution, which is only visible in the range of q below 5 nm^{-1}, is to lower the values of $c(q)$, that is to say to reduce the density fluctuations in the gas.

In that preceding work [13], we also performed MD simulations with only 256 particles. We were therefore unable to extract a correct $S(q)$ from the calculated $g(r)$. Now, we have done the simulations with a system containing 6912 particles, which is sufficient for this purpose. In order to show that the results become insensitive for large numbers of particles, we also performed a simulation with 16 384 particles. The results are essentially the same, albeit with a smaller mesh. Since the MD compare favorably to both experiments [10,12] on the small-q part of $c(q)$, it is possible to affirm without ambiguity that the interaction scheme, which consists in combining the AS two-body potential with the AT three-body contribution, is suitable for studying fluid krypton. On the other hand, the good agreement found between the HMSA and the MD attests that the self-consistent integral equation, and its extension to the three-body potentials, is very convenient. This shows once again the efficiency of the self-consistent procedure [15] at small q and reinforces our previous conclusions based on the calculation of the pair-correlation function [13].

B. Low scattering angle behavior of $c(q)$

Since the pioneering work of Johnson and March [31], it has been recognized that general features—and interesting details in some case—can be extracted from the measured structure factor. However, it has emerged that the effective potentials thus obtained are very sensitive to (i) the accuracy of the experimental data of $S(q)$ in the small-q range, and (ii) the particular liquid state theory invoked. Consequently, it can be unclear which underlying features are truly physical in origin. Formisano *et al.* [10] took advantage of the observed variations of $c(q)$ to extract useful information on the effective potential for Kr. This procedure, suggested by Reatto and Tau [32], has the merit of yielding convenient analytical expressions for certain Fourier coefficients of the small-q expansion of $c(q)$, and could provide a useful test of the asymptotic form of the integral equations, for the specific case of the dispersion forces including the three-body AT interactions.

If the structure is decided by an effective pair potential $u(r)$, it has been demonstrated in the mean spherical approximation (MSA) that the direct correlation function $c(r)$ should rapidly approach $-\beta u(r)$ for large r. According to Reatto and Tau [32], this relationship, asymptotically exact for large distance, holds quite well when the long-range dispersion term of the AS potential, $-C_6/r^6$, and the AT triple-dipole potential, $\langle u_3(r)\rangle \sim (8\pi/3)\nu\rho/r^6$, are considered. So, the direct correlation function reads

$$c(r)\sim\beta[C_6-(8\pi/3)\nu\rho]/r^6 \quad \text{as} \quad r\to\infty. \tag{19}$$

and can be predicted directly from given C_6 and ν. When using Eq. (19) and the Fourier asymptotic analysis, it is readily shown [32] that $c(q)$ has the small-q form

$$c(q)=c(0)+\gamma_2 q^2+\gamma_3|q^3|+\gamma_4 q^4+\cdots \tag{20}$$

without limitations on the integral equation used. In that expansion, it is found that γ_2 and γ_4 have no tractable expression, while γ_3 takes the simple form

$$\gamma_3=\beta(\pi^2/12)[C_6-(8\pi/3)\nu\rho]. \tag{21}$$

Thus, from the theoretical aspect, it follows that γ_3 depends linearly on the density when the AT potential is involved, whereas it is a constant in its absence. Let us expand the direct correlation function at low q, obtained with the HMSA, by extracting the coefficients γ_2, γ_3, and γ_4. To this end, $c(q)$ has been calculated at $T=297\,\mathrm{K}$ for many densities between 1.52 and 4.277 nm^{-3}, and fitted in the range between 0.5 and 5 nm^{-1} by the function Eq. (20).

Of particular interest to get additional information, and to study the relative role of the coefficients γ_2, γ_3, and γ_4, is the function

$$\lambda(q)=\frac{c(q)-c(0)}{q^2} \tag{22}$$

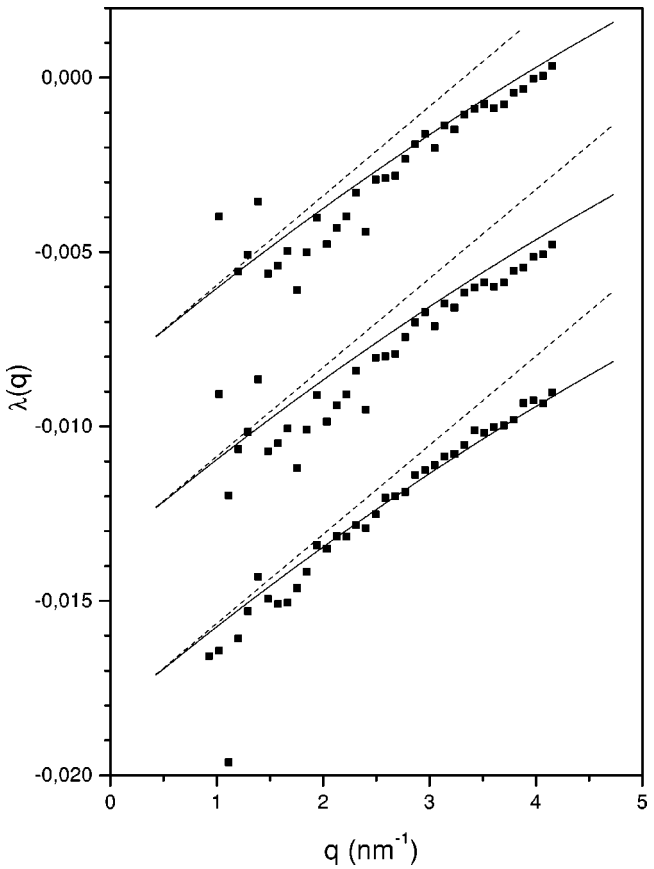

FIG. 2. Function $\lambda(q)$ for $T=297$ K at $\rho=1.52$, 1.97, and 2.42 nm^{-3} from the top to the bottom (the curves for $\rho=1.52$ and 1.97 are shifted upward by an amount of 0.005 and 0.01, respectively) calculated with the HMSA directly from the small-q expansion [Eq. (23)] (solid lines), and also from Eq. (23) in which the q^2 term was removed (dashed lines). The solid squares represent the experimental data of Formisano *et al.* [10].

that can be directly extracted from our HMSA results as well as the experimental data. In Fig. 2, we compare the theoretical curve of $\lambda(q)$ obtained from the HMSA, when the AT three-body potential is included, using Eq. (22), to the experimental data of Formisano *et al.* [10]. The results of the HMSA are in very good agreement with the experiment for all three densities. If we now express $\lambda(q)$, owing to Eq. (20), as the following function

$$\lambda(q)=\gamma_2+\gamma_3|q|+\gamma_4 q^2, \tag{23}$$

it is hardly distinguishable from the HMSA curves (not displayed in Fig. 2), showing that the expansion up to the q^2 term is sufficient. The curvature of $\lambda(q)$ at the upper q values is well reproduced revealing the presence of at least a q^4 term, while its finite limit when q tends to zero corroborates the absence of a linear term in the low-q expansion of $c(q)$ given by Eq. (20).

In order to test the linearity of the HMSA integral equation at low q, we also compare $\lambda(q)$ calculated using Eq. (22) to that obtained from Eq. (23) in which the q^2 term has been removed in Fig. 2. The merit of the latter expression is to exhibit the q^3 dependence of $c(q)$ and to reveal the range in which the q^4 term can be neglected. This is particularly important from an experimental point of view since γ_3 allows the determination of the C_6 coefficient of the London dispersion forces and the strength ν of the AT three-body potential [10,11,12] *via* Eq. (19). The curves show that the linearity of the low-q expansion of $c(q)$ is limited to a range $1<q<3$ nm^{-1}, which is slightly lower than the one estimated by Reatto and Tau [32].

C. Low-density behavior of $c(q)$

As far as the low-density behavior of the structure of Kr is concerned, the viral expansion is a valid theory with which to represent correlation functions. Neglecting terms after the first-order one in density ρ, the direct correlation function is written as [11]

$$c(q)=c_0(q)+\rho c_1(q)+O(\rho^2). \tag{24}$$

In this framework, it is useful to consider the functions $f_2(r_{ij})\{=\exp[-\beta u_2(r_{ij})]-1\}$ and $f_3(r_{ij},r_{ik},r_{jk})\{=\exp[-\beta u_3(r_{ij},r_{ik},r_{jk})]-1\}$ for the interaction scheme that combines the AS potential u_2 and the AT contribution u_3. The zeroth-order term reads

$$c_0(q)=\int f_2(r_{ij})\exp(i\mathbf{q}\cdot\mathbf{r}_{ij})d\mathbf{r}_{ij} \tag{25}$$

and the first-order one is composed of two terms

$$c_1(q)=c_1^{(2)}(q)+c_1^{(3)}(q). \tag{26}$$

While $c_1^{(2)}(q)$ depends only on u_2 as

$$c_1^{(2)}(q)=\int f_2(r_{ij})f_2(r_{ik})f_2(r_{jk})\exp(i\mathbf{q}\cdot\mathbf{r}_{ij})d\mathbf{r}_{ij}d\mathbf{r}_{ik}, \tag{27}$$

$c_1^{(3)}(q)$ contains both u_2 and u_3 contributions and reads

$$c_1^{(3)}(q)=\int [f_2(r_{ij})+1][f_2(r_{ik})+1][f_2(r_{jk})+1]f_3(r_{ij},r_{ik},r_{jk})\exp(i\mathbf{q}\cdot\mathbf{r}_{ij})d\mathbf{r}_{ij}d\mathbf{r}_{ik}. \tag{28}$$

An important feature of the low-density expansion of $c(q)$ is the presence of the function $c_1^{(3)}(q)$. Its determination represents the only way to separate the effects of the three-body effects on the correlation functions. From an experimental point of view, it has been shown very recently [11,12] that it is possible to extract $c_1^{(3)}(q_0)$ from the measurements and then to evaluate with a high degree of accuracy the strength of the AT potential.

On the theoretical side, we propose using a similar method to get the function $c_1^{(3)}(q)$ from the HMSA integral equation. First of all, we check that the HMSA numerical results of $c(q)$ are linear in density. Thus, for a given value of q, say q_0, we calculate $c(q)$ for many densities between 1.52 and 4.277 nm^{-3} and perform a linear fit that yields the values $c_0(q_0)$ and $c_1(q_0)$, which are, respectively, the ordinate at $\rho=0$ and slope of the direct correlation function. In doing so for each q of the grid, we are able to build $c_0(q)$ and $c_1(q)$ representing the low-density expansion of the HMSA. This method is applied to both results of $c(q)$, i.e., with and without the AT potential. The function $c_1^{(3)}(q)$ is finally obtained by simply subtracting $c_1(q)$ calculated with

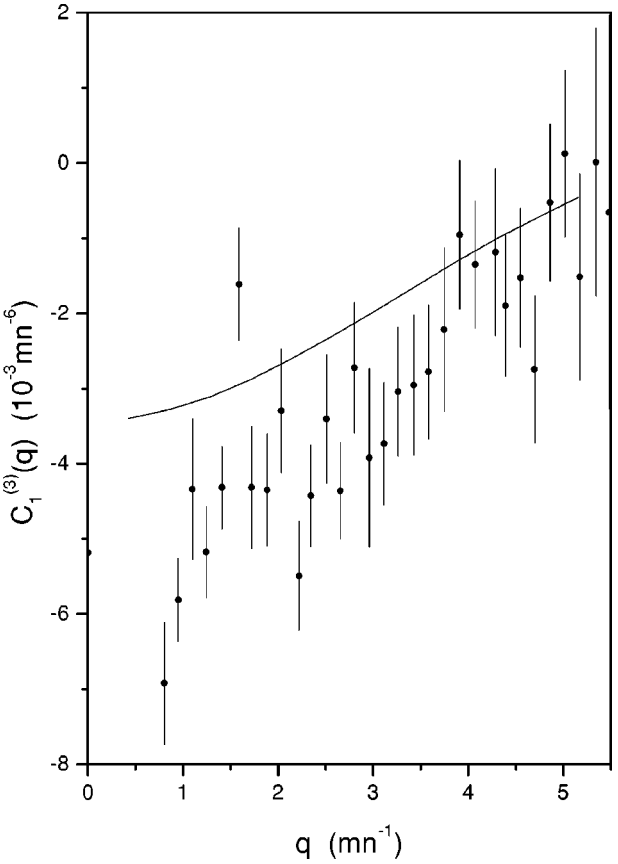

FIG. 3. Function $c_1^{(3)}(q)$ calculated from low-density expansion of the HMSA (solid lines). The solid circles with error bars stand for the experimental data of Guarini *et al.* [12].

the AS potential alone from the one including the AT contribution because, as expected, the fitted $c_0(q)$ is insensitive to the AT potential.

Figure 3 displays the theoretical and experimental curves of $c_1^{(3)}(q)$. The comparison represents probably the most stringent test for the integral equation at the three-body level. Moreover, it is relevant since Guarini *et al.* [12] have extracted their experimental data by using the same interaction model as in the present paper. An overall good agreement is seen that ensures us of the quality of the HMSA procedure. A slight overestimation appears for $q<3.5\,\mathrm{nm}^{-1}$ that can be partly interpreted by the use of a different strength ν for the three-body AT potential.

D. Thermodynamic properties

Once the inclusion of the AT potential has been shown to modify the curvature of $c(q)$ at small scattering angle, we now turn to the thermodynamic properties. A good liquid state theory and suitable interatomic interactions—particularly the three-body contribution—must be able to reproduce the well-established trends exhibited by these properties.

The excess internal energy Eq. (15) and the pressure Eq. (16)—also called the compressibility factor—are displayed in Fig. 4 as a function of density along the isotherm $T=297\,\mathrm{K}$. The calculations are performed over a wide range of densities using the HMSA for the AS potential with and

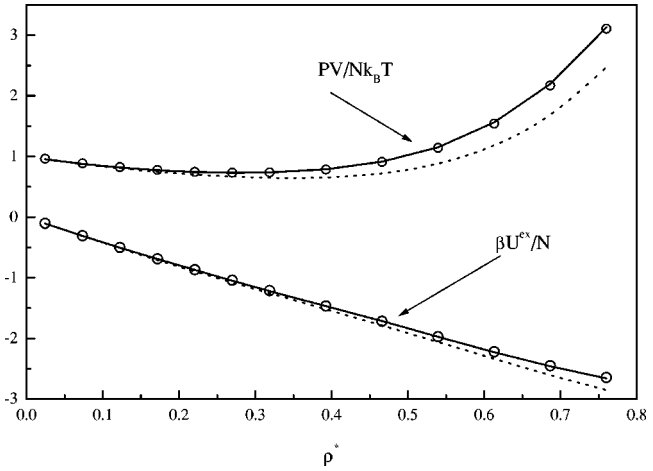

FIG. 4. Excess internal energy $\beta U^{\mathrm{ex}}/N$, and equation of state PV/Nk_BT, calculated with the HMSA integral equation for several reduced densities $\rho^*=\rho\sigma^3$ along the $T=297\,\mathrm{K}$ isotherm, by using the AS pair potential only (dotted lines) and by including the AT three-body potential (solid lines). The experimental data (open circles) are those of Trappeniers, Wassenaar, and Wolker [33].

without the AT triple-dipole interaction. As expected, the internal energy diminishes monotonically with the density, whereas the compressibility factor increases after an initial decrease underneath the ideal-gas value. For all the densities, the agreement between theory and experiment [33] is excellent when the AT contribution is included. It is worth mentioning that the positive nature of the AT potential appears clearly on both thermodynamic properties under study: the effect of the AT potential is to increase the internal energy as well as the compressibility factor compared to the AS potential alone. Moreover, its influence is somewhat larger for the pressure than for the internal energy.

Figure 5 exhibits the isothermal compressibility four different temperatures $T=273$, 297, 348, and 423 K. Our results reproduce the general tendencies of the compressibility as a function of the density: a broad maximum is located at the critical density, which gives rise to divergence as the spinodal is approached. It can be seen that the three-body

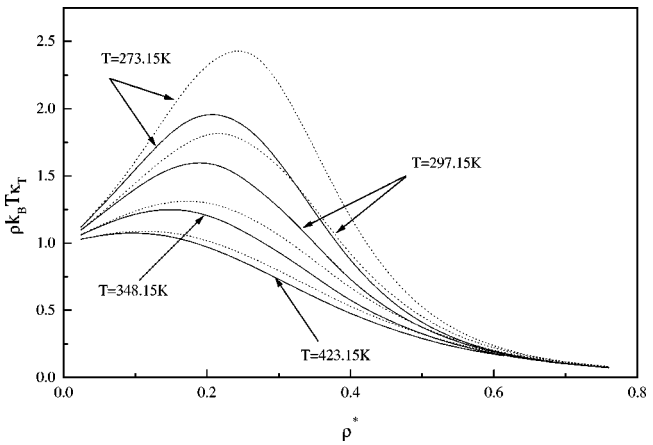

FIG. 5. Isothermal compressibility $\rho k_B T \chi_T$ for four temperatures calculated with the HMSA integral equation by using AS pair potential (dotted lines) only and by including the AT three-body contribution (solid lines).

forces have more influence when the temperature is decreasing. At a given temperature, it is shown that Kr described with the AS+AT potential is much less compressible than that modeled with the AS interaction only. This plot shows that the difference between the heights of the maxima is increasing when the temperature is becoming closer and closer to the experimental critical temperature ($T_c = 209\,\mathrm{K}$). It has been demonstrated [34] that T_c changes by about 10% due to the presence of the three-body forces, and the curves indicate that the critical temperature of the model is substantially larger than the experimental one if only two-body forces are taken into account. Therefore, the AT potential is a necessary ingredient as the critical region might be better described in this case.

The inclusion of the AT triple-dipole potential leads to an increase in the internal energy and pressure, and a decrease in the isothermal compressibility with respect to the AS potential alone. Given that the three-body AT potential is positive for most configurations of three atoms, this is not surprising. Since both AS and AT potentials behave as r^{-6} but with opposite signs at long distance [32], they tend to compensate each other and reduce the strength of the attractive tail. Therefore, the effective potential has to be taken as a whole to justify the conclusion on the isothermal compressibility. We also have to point out that the influence of the three-body AT interaction on the internal energy and the pressure becomes more significant as the density increases, while it is more important for the isothermal compressibility at intermediate densities, i.e., in the vicinity of the critical point ($\rho^* \sim 0.3$). This feature is entirely consistent with our previous calculations [13] in which the effect of AT interactions on the height of the first peak of the pair-correlation function is predominant close to the critical density.

IV. CONCLUSION

This paper is devoted to the structural and thermodynamic properties of fluid Kr. Concerning the structural properties, we have presented a comparative study on the small-q behavior of $c(q)$ for the Kr gas, at room temperature and subcritical densities. To this end, we have used interatomic interactions modelled by the two-body Aziz-Slaman potential and the three-body Axilrod-Teller potential, on one hand, and both the molecular-dynamics simulation and integral equation theory in which an effective potential combining the AS and AT potentials was constructed, on the other hand. The AS potential contains the most important dipole-dipole terms of the multipole expansion in its attractive part. In contrast, the AT term, which is an irreducible triple-dipole potential, brings a mean positive contribution that reduces the attractive tail of the full potential. The interplay between the AS and AT potentials and their respective roles in the description of the structural and thermodynamic properties of noble gases are not very well understood. This is the reason why calculations of the excess internal energy, pressure, and isothermal compressibility of Kr have been carried out over a wide range of densities.

The main feature of this paper is to notice that both experimental and theoretical approaches yield very similar results. The convergence between calculations and experiment is due to three different reasons. First, the measurements become much more precise than before, especially over that range of small q difficult to explore. Second, the fact that suitable algorithms for parallel machines enable us to perform large-scale simulation and shed much light on the behavior of correlation functions at small scattering angle. Third, HMSA is a substantial improvement of the integral equation theory, which remains a semianalytical approach competitive with the molecular dynamics.

It emerges from this paper that a very good concordance is obtained for $c(q)$ between the HMSA results, the MD simulation, and the experimental data, when the three-body AT potential is included. It has been shown that the AT potential has a small effect—though not negligible—on the small-q behavior of $c(q)$, while its presence is essential to get the correct thermodynamic properties. The main physical meaning of the AT interactions is to reduce the density fluctuations in the fluid. Thus, the agreement between the MD and experimental results demonstrates that a simple and accurate representation of the interactions for gas Kr lies in the combination of the two-body AS potential and the three-body AT contribution. The agreement between the HMSA integral equation and the experiment goes to prove that the HMSA is a competitive approach for the treatment of the structural and thermodynamic properties of the gas Kr. Therefore the present methodology could be used in the future to investigate the N-body interactions in other complex systems. However, subsequent calculations have been performed in liquid Kr near the critical temperature. Substantially, discrepancies have been seen between HMSA and MD, indicating that the HMSA extended to the three-body interactions could fail for liquid Kr near the critical point. Works are in progress along these lines. Anyway, accurate experiments are needed for these thermodynamic states in order to test the validity of the theoretical approach.

ACKNOWLEDGMENTS

The Centre Informatique National de l'Enseignement Supérieur (CINES) and the Institut de Mathématiques Appliquées de Grenoble (IMAG), where part of the numerical calculations were performed, are gratefully acknowledged for providing us with computer time. The authors would also like to thank Professor U. Bafile and Dr. E. Guarini for providing us with the experimental data of Ref. [12] prior to publication.

[1] R. A. Aziz and M. J. Slaman, Mol. Phys. **58**, 679 (1986).
[2] J. A. Barker and D. Henderson, Rev. Mod. Phys. **48**, 589 (1976).
[3] J. A. Barker, R. A. Fisher, and R. O. Watts, Mol. Phys. **21**, 657 (1971).
[4] J. A. Barker, Phys. Rev. Lett. **57**, 230 (1986).
[5] G. Casanova, R. J. Dulla, D. A. Johan, J. S. Rowlinson, and G. Savile, Mol. Phys. **18**, 589 (1970).
[6] L. Reatto and M. Tau, J. Chem. Phys. **86**, 6474 (1987).
[7] B. M. Axilrod and E. Teller, J. Chem. Phys. **11**, 299 (1943).

[8] G. A. Martynov, *Fundamental Theory of Liquids: Methods of Distribution Functions* (Adam Hilger, Bristol, 1992).
[9] R. Magli, F. Barocchi, P. Chieux, and R. Fontana, Phys. Rev. Lett. **77**, 846 (1996).
[10] F. Formisano, C. J. Benmore, U. Bafile, F. Barocchi, P. A. Egelstaff, R. Magli, and P. Verkerk, Phys. Rev. Lett. **79**, 221 (1997).
[11] C. J. Benmore, F. Formisano, R. Magli, U. Bafile, P. Verkerk, P. A. Egelstaff, and F. Barocchi, J. Phys.: Condens. Matter **11**, 3091 (1999).
[12] E. Guarini, G. Casanova, U. Bafile, and F. Barocchi, Phys. Rev. E **60**, 6682 (1999).
[13] J. M. Bomont, N. Jakse, and J. L. Bretonnet, Phys. Rev. B **57**, 10 217 (1998).
[14] G. Zerah and J. P. Hansen, J. Chem. Phys. **84**, 2336 (1986).
[15] J. L. Bretonnet and N. Jakse, Phys. Rev. B **46**, 5717 (1992).
[16] I. Charpentier and N. Jakse, Proc. SPIE **3345**, 266 (1998).
[17] C. Hoheisel, Phys. Rev. A **23**, 1998 (1981).
[18] M. Tau, L. Reatto, R. Magli, P. A. Egelstaff, and F. Barocchi, J. Phys.: Condens. Matter **1**, 7131 (1989).
[19] J. H. Kim, T. Ree, and F. H. Ree, J. Chem. Phys. **91**, 3133 (1989).
[20] P. Attard, Phys. Rev. A **45**, 3659 (1992).
[21] J. D. Weeks, D. Chandler, and H. C. Andersen, J. Chem. Phys. **54**, 4931 (1970).
[22] S. Labik, A. Malijevski, and P. Vonka, Mol. Phys. **56**, 709 (1985).
[23] J. L. Bretonnet and N. Jakse, Phys. Rev. B **50**, 2880 (1994).
[24] J. G. Kirkwood, J. Chem. Phys. **3**, 300 (1935).
[25] J. M. Haile, *Molecular Dynamics Simulation: Elementary Methods* (Wiley, New York, 1992).
[26] M. P. Allen and D. J. Tildesley, *Computer Simulation of Liquids* (Clarendon Press, Oxford, 1989); F. Yonezawa, *Molecular Dynamics Simulation* (Springer-Verlag, New York, 1992).
[27] K. Esselink, B. Smit, and P. A. J. Hilbers, J. Comput. Phys. **106**, 101 (1993); K. Esselink and P. A. J. Hilbers, *ibid.* **106**, 108 (1993).
[28] S. Plimpton, J. Comput. Phys. **117**, 1 (1995).
[29] S. Munejiri, F. Shimojo, and K. Hoshino, J. Phys.: Condens. Matter **10**, 4963 (1998).
[30] N. Jakse and I. Charpentier, Mol. Sim. (to be published).
[31] M. D. Johnson and N. H. March, Phys. Lett. **3**, 313 (1963).
[32] L. Reatto and M. Tau, J. Phys.: Condens. Matter **4**, 1 (1992).
[33] N. J. Trappeniers, T. Wassenaar, and G. J. Wolker, Physica (Amsterdam) **24**, 1503 (1966).
[34] S. Celi, L. Reatto, and M. Tau, Phys. Rev. A **39**, 1566 (1989).